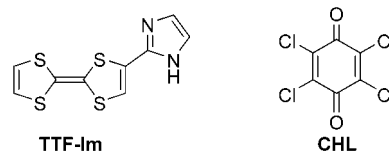


A Purely Organic Molecular Metal Based on a Hydrogen-Bonded Charge-Transfer Complex: Crystal Structure and Electronic Properties of TTF-Imidazole-*p*-Chloranil**

Tsuyoshi Murata, Yasushi Morita,* Kozo Fukui, Kazunobu Sato, Daisuke Shiomi, Takeji Takui, Mitsuhiro Maesato, Hideki Yamochi, Gunzi Saito,* and Kazuhiro Nakasuji*

The control of the relative molecular orientation of redox-active molecules is of great importance for constructing organic conductors and superconductors.^[1] Ingenious manipulation of noncovalent interactions such as hydrogen bonding (H-bonding) is an efficient tool for creation of desired molecular arrangements.^[2] Thus, a variety of tetrathiafulvalene (TTF) derivatives with H-bonding functionality have been synthesized.^[3] However, most of these gave insulating or semiconducting charge-transfer (CT) complexes and salts,^[3] while CT salts of ethylenedithio-TTF-CONHMe with inorganic anions solely exhibited metallic behavior.^[3c,d] The imidazole ring system has been utilized as an interesting building block for H-bonded CT complexes^[4] and assembled metal complexes.^[5] Recently, we have designed TTF derivatives substituted with an imidazole moiety, TTF-Im, for exploring molecular conductors with highly ordered molecular aggregation by H-bonding.^[6] We report here the first purely organic molecular metal based on the H-bonded CT complex composed of TTF-Im and *p*-chloranil (CHL), in

which the component ratio and electron-accepting ability of CHL are controlled by H-bonding.^[7]



In CV measurements, TTF-Im shows the first oxidation potential at -0.06 V vs Fc/Fc^+ , which is close to that of TTF (-0.09 V).^[6] Single crystals of TTF-Im were obtained by the vapor diffusion method with hexane/THF.^[8] In the crystal structure of TTF-Im, the imidazole moiety is twisted by $15.5(1)^\circ$ from the TTF skeleton. The imidazole ring forms a one-dimensional chain by $\text{N}-\text{H}\cdots\text{N}$ H-bonding interaction (3.06 Å) along the *a* axis in a zigzag fashion similar to that of imidazole^[9] (Figure 1). The TTF-Im molecule uniformly

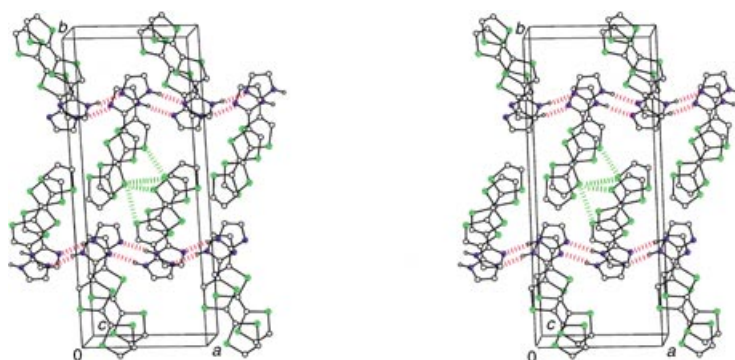


Figure 1. Stereoview of the crystal packing of TTF-Im, showing $\text{N}-\text{H}\cdots\text{N}$ H-bonding (red), π -stacking columns, and $\text{S}\cdots\text{S}$ contacts (green) between columns.

stacks and forms a columnar structure parallel to the *c* axis with a face-to-face distance of 3.66 Å. The column is connected by H-bonding and intercolumnar $\text{S}\cdots\text{S}$ contacts (3.48 and 3.57 Å) along the *a* axis (Figure 1) to give a three-dimensional network.

The CT complex $(\text{TTF-Im})_2(\text{CHL})$ was obtained as black needlelike crystals by diffusion of a solution of TTF-Im and CHL in acetonitrile containing 2 vol % ethanol in an H-shaped tube.^[7,10,11] The $\text{C}=\text{O}$ stretching frequency of 1532 cm^{-1} in the IR spectrum indicates that the CHL molecule exists as a radical anion.^[12] Thus, the ionicity of TTF-Im is estimated to be $+0.5$.^[13] Crystal structure analysis shows that the molecular structure of TTF-Im is nearly planar, with a small dihedral angle of $5.5(1)^\circ$ between the TTF and imidazole moieties, and the CHL molecule lies on the inversion center (Figure 2). The CHL forms a bifurcated triad with two TTF-Im molecules through double $\text{N}-\text{H}\cdots\text{O}$ H-bonding interactions. Because these H-bonds increase the electron-accepting ability of the CHL molecule, the CHL in the complex is a completely one-electron reduced.^[14] Each component molecule forms a uniform stacking column along the *a* axis with interplanar distances of 3.46 Å for TTF-Im and 3.19 Å for CHL. Furthermore, side-by-side $\text{S}\cdots\text{S}$ contacts

[*] T. Murata, Prof. Dr. Y. Morita, Prof. Dr. K. Nakasuji
Department of Chemistry, Graduate School of Science
Osaka University
Toyonaka, Osaka 560-0043 (Japan)
Fax: (+81) 6-6850-5395
E-mail: morita@chem.sci.osaka-u.ac.jp

Prof. Dr. M. Maesato, Prof. Dr. G. Saito
Division of Chemistry, Graduate School of Science
Kyoto University
Sakyo-ku, Kyoto 606-8502 (Japan)
Fax: (+81) 75-753-4035

Prof. Dr. K. Sato, Prof. Dr. D. Shiomi, Prof. Dr. T. Takui
Departments of Chemistry and Materials Science
Graduate School of Science
Osaka City University
Sumiyoshi-ku, Osaka 558-8585 (Japan)

Prof. Dr. H. Yamochi
Research Center for Low Temperature and Materials Science
Kyoto University
Sakyo-ku, Kyoto 606-8502 (Japan)
Prof. Dr. Y. Morita, Dr. K. Fukui
PRESTO, JST (Japan)

[**] This work was partially supported by PRESTO-JST, and by 21COE program "Creation of Integrated EcoChemistry of Osaka University".

Supporting information for this article is available on the WWW under <http://www.angewandte.org> or from the author.

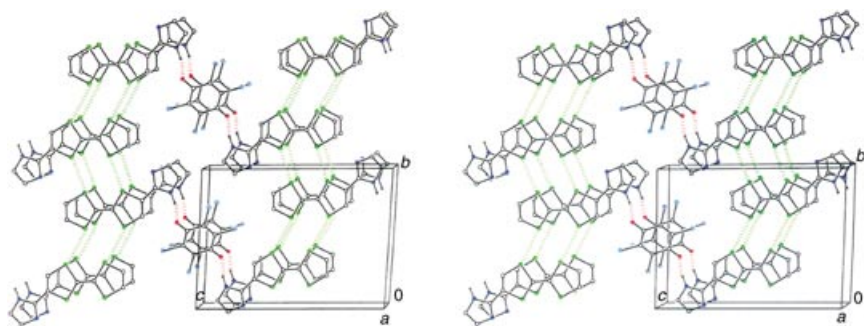


Figure 2. Stereoview of the crystal packing of (TTF-Im)₂(CHL). The dashed lines show the intermolecular interactions: N–H...O H-bonding (red) and S...S contacts (green).

between TTF columns (3.51–3.57 Å) along the *b* axis form a two-dimensional donor layer parallel to the *ab* plane. Together with the double H-bonding of CHL, this results in a three-dimensional network of intermolecular interactions in the crystal.

Intermolecular overlap integrals of the HOMO of the donor molecules in the CT complex, calculated by the extended Hückel method, are summarized in Figure 3a.^[15]

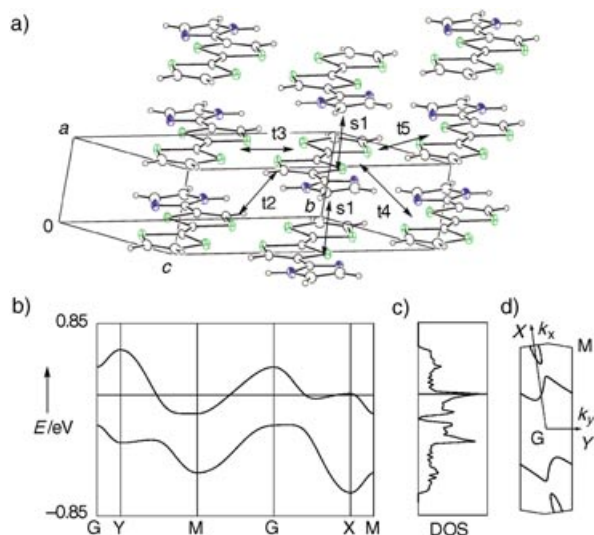


Figure 3. a) Packing pattern of the donor molecules; letters indicate intermolecular overlap integrals ($s_1 = -20.77$, $t_2 = 0.94$, $t_3 = -5.44$, $t_4 = 10.73$, $t_5 = -0.62$). b) Energy dispersion, c) density of states, and d) Fermi surface of (TTF-Im)₂(CHL), calculated by the extended Hückel method with tight-binding approximation.

Although the strongest overlap integral (s_1) was observed along the stacking direction, interactions on the same order of magnitude (t_3 , t_4) were also calculated in the side-by-side directions. The tight-binding approximation gave the energy dispersion, density of states, and Fermi surfaces shown in Figure 3b–d. As shown in Figure 3b, the dispersion affords two bands having a gap of 0.05 eV, the upper one of which is half-filled. The main parts of the Fermi surfaces in Figure 3d exhibit a strongly warped one-dimensional feature. Along with these open surfaces, a hole pocket around point X was derived.

The static paramagnetic susceptibility χ_p of the polycrystalline sample showed nearly temperature-independent behavior in the range of 170–350 K, and its value of $+5.7 \times 10^{-4} \text{ emu mol}^{-1}$ per (TTF-Im)₂(CHL) unit is consistent with Pauli paramagnetism (Figure 4). The χ_p value slightly decreased below 170 K, and after passing through a minimum at 90 K, a strongly temperature-dependent component appeared to increase the total χ_p in the lower temperature region (Figure 4). The magnetic field dependence of the magnetization at 1.9 K revealed that the temperature-dependent part of

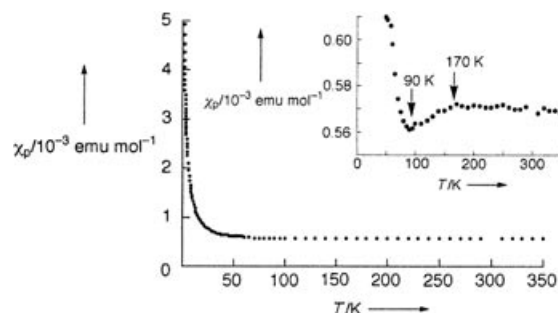


Figure 4. Temperature dependence of magnetic susceptibility after correction of Pascal diamagnetism for a polycrystalline sample of (TTF-Im)₂(CHL). The inset shows a magnification of the plot.

χ_p is attributed to 1.1 % of nearly isolated $S = 1/2$ spins.^[16] No such temperature-dependent contribution was observed above 170 K, and this suggests that the generation of such a component may be associated with the subtle anomaly around 90–170 K.

The ESR spectra of the polycrystalline sample at 296 K showed a single Lorentzian absorption with $g = 2.0068$ (Figure 5). The ESR linewidth ΔB ^[17] steadily decreased on lowering the temperature (inset to Figure 5) and finally became sharp enough to resolve g anisotropy as (g_{xx} , g_{yy} , g_{zz}) =

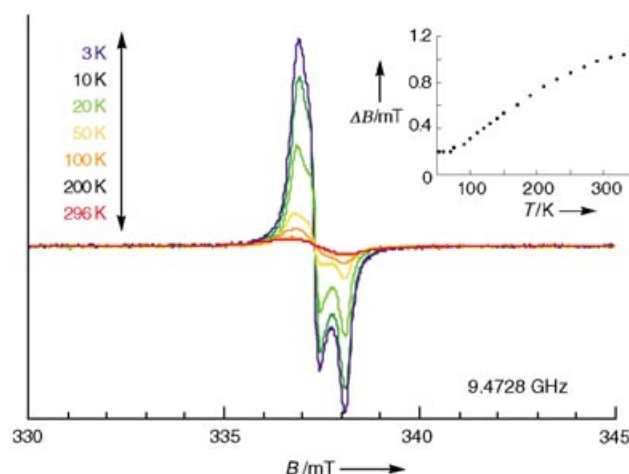


Figure 5. Temperature dependence of ESR spectra for a polycrystalline sample of (TTF-Im)₂(CHL). The inset shows the temperature dependence of ESR linewidth ΔB .^[17]

(2.0101, 2.0075, 2.0028), which are characteristic values of TTF⁺ derivatives. The ESR signal intensity exhibits nearly identical behavior to χ_p at all temperatures. The above results show that the TTF-Im column acts a pathway for electrical conduction. In contrast, no ESR absorption originating from uniformly stacked CHL⁻ molecules was observed, probably because the short interplane distance of CHL⁻ (3.19 Å) and the large orbital overlaps induce a strong antiferromagnetic interaction that quenches paramagnetism. Density functional theory calculations gave support to this conjecture. For a pair of CHL⁻ molecules in the uniform column taken from the X-ray structure, the exchange coupling was calculated to be $2J/k_B = -2677$ K,^[18] which results in negligible paramagnetic contribution below 350 K as long as a one-dimensional magnetic chain is considered (Bonner–Fisher model^[19]).

The temperature dependence of electrical conductivity for the single crystal along the π -stacking direction confirms metallic behavior down to about 180 K, below which the resistivity increases gradually (activation energy 20 meV; Figure 6). The room-temperature electrical conductivity of

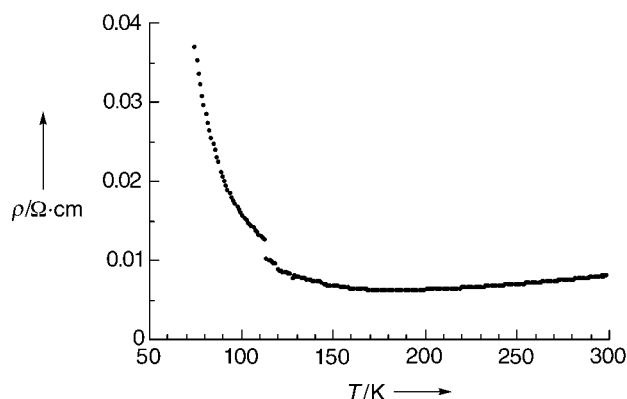


Figure 6. Temperature dependence of electrical resistivity of (TTF-Im)₂(CHL) measured by the four-probe method along the long axis (*a* axis) of a needlelike crystal.

this complex of $\sigma_{\text{rt}} = 124$ S cm⁻¹ is comparable to those of CT salts of ethylenedithio-TTF-CONHMe^[3c,d] and TTF-TCNQ complexes,^[20] and 10⁴–10⁷ orders of magnitude higher than those of CT complexes with organic electron acceptors based on H-bonded TTF derivatives.^[3] Clarification of the subtle anomaly in magnetic and electric properties at 90–180 K is the subject of further study.

In conclusion, we have prepared the first purely organic molecular metal based on an H-bonded CT complex. The absence of an abrupt change like the Peierls transition shows that the H-bonding interaction plays a vital role in transport properties by increasing dimensionality. Furthermore, we emphasize the ability of H-bonding interactions to control the electron-accepting ability of CHL and the donor/acceptor ratio by the formation of H-bonded triad of TTF-Im and CHL. We believe that these salient features of H-bonding interactions in purely organic CT complexes demonstrate a new concept for the molecular design of organic conductors.^[21]

Received: May 27, 2004

Keywords: conducting materials · crystal engineering · hydrogen bonds · magnetic properties

- a) M. R. Bryce, *J. Mater. Chem.* **1995**, 5, 1481; b) P. Batail, K. Boubekeur, M. Fourmigué, J.-C. P. Gabriel, *Chem. Mater.* **1998**, 10, 3005.
- For a recent overview of H-bonding, see *The Weak Hydrogen Bond* (Eds.: G. R. Desiraju, T. Steiner), Oxford University Press, New York, **1999**, chap. 1.
- Examples of H-bonded TTF derivatives: Hydroxymethyl: a) P. Blanchard, K. Boubekeur, M. Sallé, G. Duguay, M. Jubault, A. Gorgues, J. D. Martin, E. Canadell, P. Auban-Senzier, D. Jérôme, P. Batail, *Adv. Mater.* **1992**, 4, 579. Carboxy: b) A. Dolbecq, M. Fourmigué, P. Batail, *Bull. Soc. Chim. Fr.* **1996**, 133, 83; Amide: c) K. Heuzé, C. Mézière, M. Fourmigué, P. Batail, C. Coulon, E. Canadell, P. Auban-Senzier, D. Jérôme, *Chem. Mater.* **2000**, 12, 1898; d) K. Heuzé, M. Fourmigué, P. Batail, E. Canadell, P. Auban-Senzier, *Chem. Eur. J.* **1999**, 5, 2971; e) S. A. Baudron, N. Avarvari, P. Batail, C. Coulon, R. Clérac, E. Canadell, P. Auban-Senzier, *J. Am. Chem. Soc.* **2003**, 125, 11 583. Thioamide: f) A. J. Moore, M. R. Bryce, A. S. Batsanov, J. N. Heaton, C. W. Lehmann, J. A. K. Howard, N. Robertson, A. E. Underhill, I. F. Perepichka, *J. Mater. Chem.* **1998**, 8, 1541. Nucleic acid: g) Y. Morita, S. Maki, M. Ohmoto, H. Kitagawa, T. Okubo, T. Mitani, K. Nakasuji, *Org. Lett.* **2002**, 4, 2185. Pyrrole-fused: h) K. Zong, W. Chen, M. P. Cava, R. D. Rogers, *J. Org. Chem.* **1996**, 61, 8117; i) J. O. Jeppesen, K. Takimiya, F. Jensen, T. Brimert, K. Nielsen, N. Thorup, J. Becher, *J. Org. Chem.* **2000**, 65, 5794; j) K. A. Nielsen, J. O. Jeppesen, E. Levillain, J. Becher, *Angew. Chem.* **2003**, 115, 197; *Angew. Chem. Int. Ed.* **2003**, 42, 187; for a review, see: k) J. O. Jeppesen, J. Becher, *Eur. J. Org. Chem.* **2003**, 3245. Uracil-fused: l) O. Neilands, S. Belyakov, V. Tilika, A. Edzina, *J. Chem. Soc. Chem. Commun.* **1995**, 325; m) O. Neilands, V. Liepinsh, B. Turovska, *Org. Lett.* **1999**, 1, 2065; n) K. Balodis, S. Khasanov, C. Chong, M. Maesato, H. Yamochi, G. Saito, O. Neilands, *Synth. Met.* **2003**, 133–134, 353.
- a) T. Akutagawa, G. Saito, *Bull. Chem. Soc. Jpn.* **1995**, 68, 1753; b) T. Akutagawa, G. Saito, M. Kusunoki, K. Sakaguchi, *Bull. Chem. Soc. Jpn.* **1996**, 69, 2487.
- a) M. Tadokoro, H. Kanno, T. Kitajima, H. S. Umemoto, N. Nakanishi, K. Isobe, K. Nakasuji, *Proc. Natl. Acad. Sci. USA* **2002**, 99, 4950; b) Y. Morita, T. Murata, K. Fukui, M. Tadokoro, K. Sato, D. Shiomi, T. Takui, K. Nakasuji, *Chem. Lett.* **2004**, 33, 188.
- Y. Morita, T. Murata, H. Yamochi, G. Saito, K. Nakasuji, *Synth. Met.* **2003**, 135–136, 579. See also the Supporting Information.
- TTF-CHL is a neutral CT complex with 1:1 component ratio and is a semiconductor with low electrical conductivity ($\sigma_{\text{rt}} = \sim 10^{-4}$ S cm⁻¹): J. B. Torrance, J. J. Mayerle, V. Y. Lee, K. Bechgaard, *J. Am. Chem. Soc.* **1979**, 101, 4747.
- Crystal data for TTF-Im: C₉H₆N₂S₄, $M_r = 270.40$, crystal dimensions $0.25 \times 0.15 \times 0.05$ mm³, orthorhombic, space group *Pna*2₁ (no. 33), $a = 10.198(1)$, $b = 25.196(4)$, $c = 4.1681(5)$ Å, $V = 1071.0(2)$ Å³, $Z = 4$, $\rho_{\text{calcd}} = 1.677$ g cm⁻³, $\mu = 8.49$ cm⁻¹, $2\theta_{\text{max}} = 55.0^\circ$, $\lambda(\text{MoK}\alpha) = 0.71075$ Å, ω scan mode, $T = 200$ K, 9749 reflections, of which 2853 were unique and 2116 were included in the refinement [$I > 2.00\sigma(I)$], data corrected for Lorentzian and polarization effects; an empirical absorption correction resulted in transmission factors ranging from 0.8302 to 0.9582, solution by direct methods (MITHRIL 90) and refinement on $|F^2|$ by full-matrix least-squares procedures (SHELXL97), 136 parameters, the non-H atoms were refined anisotropically, H atoms were included but not refined, final values $R_1 = 0.032$, $wR_2 = 0.069$, GOF = 1.06, maximum positive and negative peaks in ΔF map were $\rho_{\text{max}} = 0.26$ e Å⁻³ and $\rho_{\text{min}} = -0.21$ e Å⁻³. CCDC-239640 contains the supplementary crystallographic data for this

paper. These data can be obtained free of charge via www.ccdc.cam.ac.uk/conts/retrieving.html (or from the Cambridge Crystallographic Data Centre, 12, Union Road, Cambridge CB21EZ, UK; fax: (+44)1223-336-033; or deposit@ccdc.cam.ac.uk).

- [9] a) S. Martinez-Carrera, *Acta Crystallogr.* **1966**, *20*, 783; b) B. M. Craven, R. K. McMullan, J. D. Bell, H. C. Freeman, *Acta Crystallogr. Sect. B* **1977**, *33*, 2585.
- [10] Crystal data for (TTF-Im)₂(CHL): C₁₂H₆N₂OS₄Cl₂, *M_r* = 393.34, crystal dimensions 0.30 × 0.05 × 0.02 mm³, triclinic, space group *P* $\bar{1}$ (no. 2), *a* = 3.7573(2), *b* = 12.2435(4), *c* = 15.8037(5) Å, α = 93.996(3), β = 85.915(3), γ = 82.138(3)°, *V* = 716.02(5) Å³, *Z* = 2, ρ_{calcd} = 1.824 g cm⁻³, μ = 95.20 cm⁻¹, $2\theta_{\text{max}}$ = 55.0°, $\lambda(\text{CuK}\alpha)$ = 1.54178 Å, ω scan mode, *T* = 293 K, 8786 reflections, of which 2521 were unique and 7895 were included in the refinement [*I* > 2.00σ(*I*)], data corrected for Lorentzian and polarization effects; an empirical absorption correction resulted in transmission factors ranging from 0.7196 to 1.0000, solutions by direct methods (SIR 97) and refinement on $|F^2|$ by full-matrix least-squares procedures, 192 parameters, the non-H atoms were refined anisotropically, H atoms were included but not refined, final values *R*₁ = 0.058, *wR*₂ = 0.171, GOF = 1.068, maximum positive and negative peaks in ΔF map were ρ_{max} = 0.42 e Å⁻³ and ρ_{min} = -0.42 e Å⁻³. CCDC 239641 contains the supplementary crystallographic data for this paper. These data can be obtained free of charge via www.ccdc.cam.ac.uk/conts/retrieving.html (or from the Cambridge Crystallographic Data Centre, 12, Union Road, Cambridge CB21EZ, UK; fax: (+44)1223-336-033; or deposit@ccdc.cam.ac.uk).
- [11] Selected physical data: (TTF-Im)₂(CHL), IR (KBr): $\tilde{\nu}$ = 3200–2700, 1532 cm⁻¹; UV/Vis (KBr): λ_{max} = 290, 386, 700, 834 nm; elemental analysis (%): calcd for (C₉H₆N₂S₄)₂(C₆O₂Cl₄): C 36.64, H 1.54, N 7.12; found: C 36.77, H 1.57, N 7.22.
- [12] A. Girlando, I. Zanon, R. Bozio, C. Pecile, *J. Chem. Phys.* **1978**, *68*, 22.
- [13] (TTF-Im)₂(CHL) shows the lower-energy absorption band at around 3000 cm⁻¹, which is characteristic of partial CT complexes with segregated stacking columns (see the Supporting Information).
- [14] The oxidation potential of TTF-based donor molecules with an amido moiety is strongly affected by formation of H-bonds to inorganic anions.^[3c]
- [15] Calculation method: T. Mori, A. Kobayashi, Y. Sasaki, H. Kobayashi, G. Saito, H. Inokuchi, *Bull. Chem. Soc. Jpn.* **1984**, *57*, 627.
- [16] The amount of the temperature-dependent contribution, 1.1 %, was determined by the saturation magnetization at 1.9 K (123.01 erg Oe⁻¹ mol⁻¹) under the assumption that a unit of (TTF-Im)₂(CHL) has nominally two *S* = 1/2 spins by complexation.
- [17] The ESR spectra observed at all temperatures were reproduced by spectral simulation for a randomly oriented system, which assumes temperature-independent *g* anisotropy (see text) and temperature-dependent peak-to-peak linewidths (inset of Figure 5).
- [18] The 2*J* value was calculated at the UB3LYP/6-31G(d) level according to the procedure developed by Yamaguchi et al.: Y. Takano, T. Taniguchi, H. Isobe, T. Kubo, Y. Morita, K. Yamamoto, K. Nakasuji, T. Takui, K. Yamaguchi, *J. Am. Chem. Soc.* **2002**, *124*, 11122, and references therein.
- [19] J. C. Bonner, M. E. Fisher, *Phys. Rev. A* **1964**, *135*, 640.
- [20] R. P. Groff, A. Suna, R. E. Merrifield, *Phys. Rev. Lett.* **1974**, *33*, 418.
- [21] A phase transition in H-bonded CT complex: K. Nakasuji, K. Sugiura, T. Kitagawa, J. Toyoda, H. Okamoto, K. Okaniwa, T. Mitani, H. Yamamoto, I. Murata, A. Kawamoto, J. Tanaka, *J. Am. Chem. Soc.* **1991**, *113*, 1862.